

Extracting contact forces in bonded granular ensembles

Abrar Naseer^{1,*}, Karen E. Daniels^{2,**}, and Tejas G. Murthy^{1,***}

¹Department of Civil Engineering, Indian Institute of Science, Bangalore, India

²Department of Physics, North Carolina State University, Raleigh, NC, USA

Abstract. Interparticle bonding is prevalent in stored powders, geological formations, and infrastructure engineering, yet a comprehensive understanding of the effects of its micro-mechanics on bulk properties has not been established experimentally. One challenge has been that while photoelasticity has been widely and successfully used to measure the vector contact forces within dry granular systems, where the particle-particle interactions are solely frictional and compressive in nature, it has seen little development in systems where tensile forces are present. The key difficulty has been the inability to distinguish between compressive and tensile forces, which appear identically within the photoelastic response.

Here, we present a novel approach which solves this problem, by an extension to the open-source PeGS (Photoelastic Grain Solver) software available at <https://github.com/photoelasticity>. Our new implementation divides the procedure of finding vector contact forces into two steps: first evaluating the vector contact forces on the non-bonded particles present in the ensemble, followed by using an equilibrium constraint to solve for the forces in the bonded particles. We find that in the dilute limit, for up to 25% bonded dimers, we can solve for all forces since each particle has only one force bearing contact that can potentially transmit tensile forces. While the case of dimers is an idealised version of bonded granular ensemble, it provides an important first step towards experimentally studying the micro-mechanics of bonded granular materials.

1 Introduction

Photoelasticity has found wide use in the study of granular materials. After pioneering work by Wakabayashi [1], Majmudar & Behringer [2] solved the inverse problem to obtain vector contact forces using photoelasticity, paving the way for numerous quantitative, micro-mechanical studies on granular materials. This quantification of vector contact forces has led to exploration of chute flows [3], the yielding transition [4], shape effects [5, 6], force responses under varied boundary conditions [7], rigidity percolation [8], and shear jamming [9] in granular materials. However, for many years the use of photoelastic techniques [10, 11] has focused on the properties and behaviour of non-bonded granular materials, leaving bonded granular materials relatively unexplored.

Yet, interparticle bonding [12] is a widely encountered phenomenon in granular materials. In the presence of bonding, the resistance of the granular material to shear and tensile forces improves drastically [13–15]. The effect of bonding on the granular materials has been well studied using ensemble-level experiments [13, 16] as well as the discrete element method (DEM) simulations [5, 17]. To extend the use of photoelasticity to bonded granular materials, we put forward an approach which extends an existing, open source method [18] of obtaining vector contact forces in granular materials to solve for dilute tensile

forces. After describing how bonding complicates the contact force extraction process, we present a method for overcoming these challenges, demonstrate that it works for dilute bonding, and illustrate its effects on system-wide force transmission.

2 Photoelastic methods

The current implementation of photoelasticity [19, 20] in non-bonded granular materials is well established for 2D planar systems and derives the vector contact forces [10, 11] under the assumption that only compressive (non-tensile) forces are present, but those arising due to bonding remain unexplored. When tensile forces are present, as is the case for bonded granular materials, this creates an ambiguity in the method since normal contact forces f_n and $-f_n$ create identical photoelastic responses. This is illustrated in Figure 1, which compares the expected fringe pattern formed in a bonded pair of particles under diametric compressive and tensile loading. This arises because the stress field inside the particles results in the fringe pattern governed by

$$I(x, y) = I_0 \sin^2 \left(\frac{\pi(p - q)hC}{\lambda} \right) \quad (1)$$

where I_0 is the overall light intensity, (p, q) are the principal stresses, h is the particle thickness, $C(\lambda)$ is the wavelength-dependent stress-optic coefficient and λ is the wavelength of the polarised light. Because $p(x, y)$ and

*e-mail: abrarnaseer@iisc.ac.in

**e-mail: kdaniel@ncsu.edu

***e-mail: tejas@iisc.ac.in

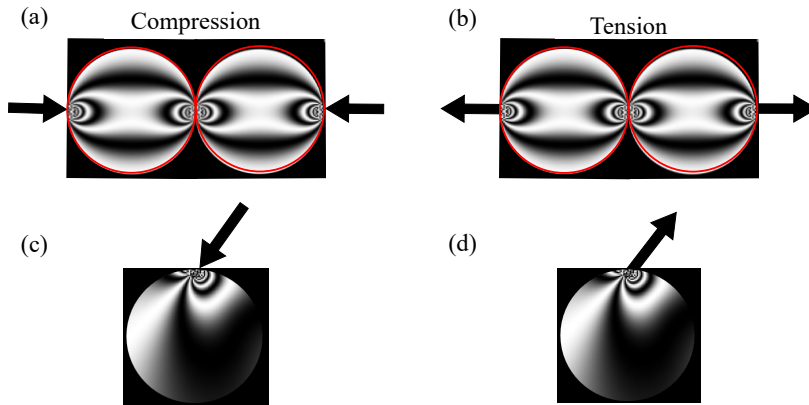


Figure 1. Numerically solutions comparing the resulting fringe pattern for compression (left) and tension (right) under the inversion $f_n = -f_n$. Top row: diametric loading (no tangential forces). Bottom rows: the contribution from a single contact with the same tangential force.

$q(x, y)$ are identical under an inversion of the normal force, Eq. 1 does not distinguish the compressive and tensile cases.

Prior work has focused on dry granular materials, for which the PeGS algorithm uses an inverse mapping and optimization procedure which always selects the compressive force instead of the tensile force when solving for the normal force. The sensitivity to parameter choices has been well-documented [8, 21] for that case, but since the possibility of tensile forces creates an indeterminacy in the sign of the normal force which cannot be determined by this inverse process, additional information is required to select the correct solution. In general, forces are not colinear, as illustrated for a single frictionally-loaded contact in Fig. 1, for which the frictional contact could be either compressive or tensile and yet have the same fringe pattern. As we will see below, establishing torque and force balance within a bonded system is able to resolve this indeterminacy.

3 Introducing interparticle bonds

We develop and test our new methods using experiments on a quasi-two-dimensional packing of photoelastic grains

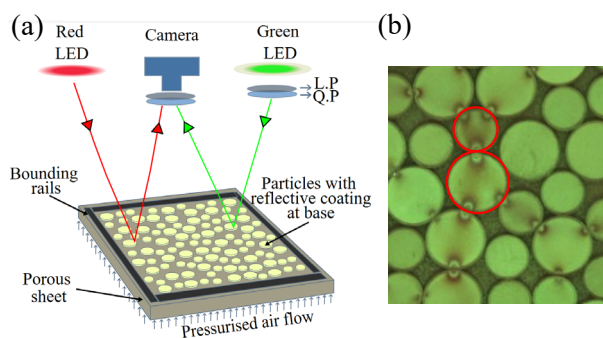


Figure 2. (a) Schematic of the experimental setup: the red LED is used for particle detection, while a polarized green LED is used to visualize the fringe pattern in the loaded ensemble. (b) A subsection of the experiment shows a cluster of photoelastic particles with a pair of particles (marked with red circles) bonded together.

with controlled, dilute bonding. Our particles rest above a horizontal porous sheet which floats them on a gentle layer of pressurised air (see Fig. 2a), reducing the effects of basal friction on the force transmission. The particles are photoelastic (Vishay PSM-4) and are visualized within a brightfield polariscope. The combination of the linear polarizer (LP) and quarter plate (QP) placed in front of the green light source and the overhead camera is used to extract the force network by rotation of the polarisation of the green light. We introduce bonding by randomly cohering pairs of particles with white glue at fixed locations which we identify in advance. To load the sample and create a force network, we provide a small amount of biaxial compression from two of the walls; a subregion of the granular material containing a bonded pair is shown in Figure 2b.

To obtain the vector contact forces and hence a well-matched pseudo-image in a bonded granular material, we divide the procedure into three steps. In the very first step, we locate the particles that are bonded in the ensemble by assigning them unique IDs for detection in the ensemble. In Fig. 3a, this is shown by two circles circumscribing the bonded pair. For all particles except the bonded ones, the PeGS data analysis pipeline proceeds as usual, since none of these will contain tensile forces. Since PeGS evaluates vector contact forces particle-wise, this removal of bonded particles does not affect the convergence procedure for the non-bonded particles. This process is illustrated in the reconstructed pseudo image in Fig. 3b. Next, we evaluate forces on all the neighbouring particles of the bonded pairs: by Newton’s Third Law (reciprocity), this determines the external forces acting on each of the bonded particles, as shown in Fig. 3c. Finally, by invoking force and torque balance on the individual particles, we can solve for the contact force (f_x, f_y) transmitted through the bond itself. As shown in Fig. 3d, the reconstructed fringe pattern in the bonded pair matches well with its experimental image. It should be noted that while solving for the normal and tangential components, the force-bearing contacts follow a calibrated force model based on linear elasticity, as mentioned in Ref. [10, 11].

Therefore, we find that by separating the process of extracting the vector contact forces into two steps — first, analyzing the non-bonded particles, and second, handling the bonded particles — we can reconstruct a combined image

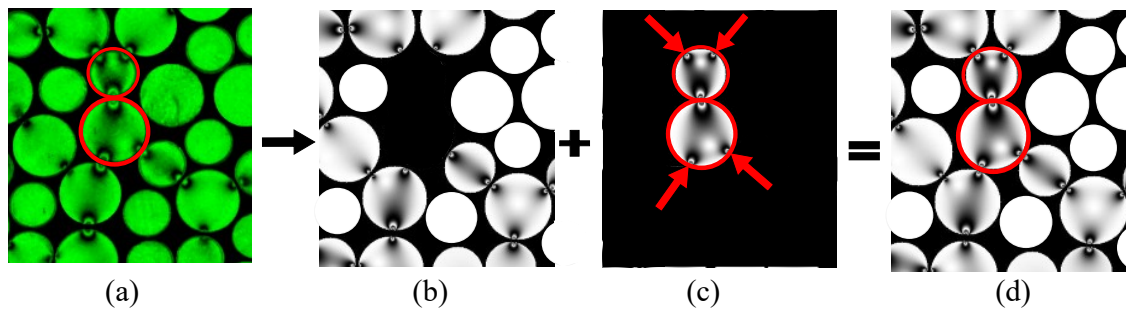


Figure 3. Summary of the steps from an image to solved contact forces. Bonded particles (a) are initially removed from the analysis (b), after which they are solved using the forces (c) from their neighboring particles, to create the final result (d).

that accurately represents the complete pseudo-image of the experimental image. Note that this result neglects the smallest forces, for which the fringe pattern may have an intensity below the threshold used to detect force-bearing contacts. This process has been successful in processing granular materials with up to 25% bonded pairs [22]. An example is shown in Fig. 4 where the entire bonded ensemble is biaxially compressed, resulting in the formation of force network. In addition to compressive forces, the vector force data reveals the presence of tensile interactions at the bonds (Fig. 4b). Particle pairs shown in red colour are the ones experiencing net tensile forces through their interparticle bonds, whereas those in blue colour experience net compressive forces. This finding opens the regime of comprehensive experimental study of the particle-level features of bonded granular ensembles.

4 Conclusion

Our new implementation [23], soon to be included in the new release of PeGS [24], allows us to extend photoelastic techniques to work on bonded granular materials. This procedure will likely also apply to systems where particles are bonded in longer linear structures, or even to larger clusters by starting from the edges (only one bond/particle) and working inwards iteratively. Our model bonds closely resemble any bond that has a rigidity similar to the particle rigidity, such as cementation, solid bridges, or a polymer coating. Our improvement will enable future work on the micro-mechanics of bonded granular materials.

5 Acknowledgments

We are grateful to funding from the National Science Foundation (DMR-2104986), Anusandhan National Research Foundation (ANRF-CRG/2022/003750) and the Fulbright-Nehru fellowship program.

References

[1] T. Wakabayashi, Photo-elastic method for determination of stress in powdered mass, *Journal of the Physical Society of Japan* **5**, 383 (1950).

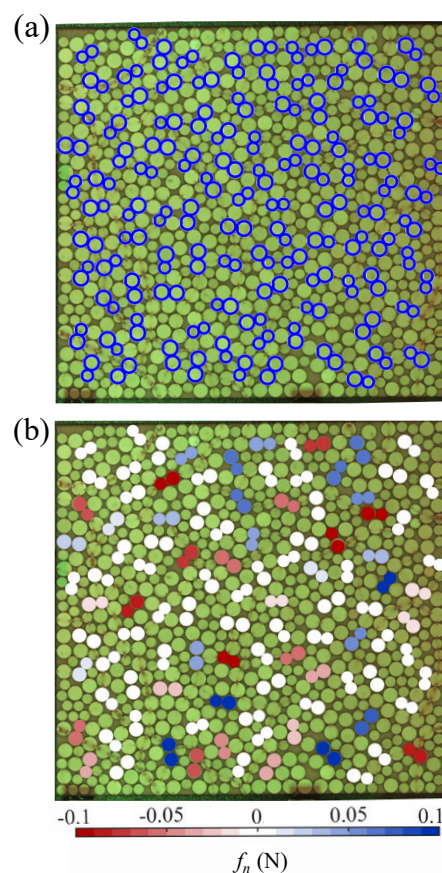


Figure 4. Example of (a) a fully-solved granular packing with 25% bonded pairs (shown by blue outlines), and the resulting force network and (b) the fluctuating nature of normal force (f_n) transmitting through the bonds. The coloured pairs are the bonded particles, where particles in the red spectrum bear tensile forces, and in the blue are compressed.

[2] T.S. Majmudar, R.P. Behringer, Contact force measurements and stress-induced anisotropy in granular materials, *nature* **435**, 1079 (2005).
 [3] A.L. Thomas, N.M. Vriend, Photoelastic study of dense granular free-surface flows, *Physical Review E* **100**, 012902 (2019).

- [4] J. Shang, Y. Wang, D. Pan, Y. Jin, J. Zhang, The yielding of granular matter is marginally stable and critical, *Proceedings of the National Academy of Sciences* **121**, e2402843121 (2024).
- [5] Y. Wang, S. Leung, Characterization of cemented sand by experimental and numerical investigations, *Journal of geotechnical and geoenvironmental engineering* **134**, 992 (2008).
- [6] Y. Wang, J. Shang, Y. Wang, J. Zhang, Contact force measurements and local anisotropy in ellipses and disks, *Physical Review Research* **3**, 043053 (2021).
- [7] L. Zhang, Y. Wang, J. Zhang, Force-chain distributions in granular systems, *Physical Review E* **89**, 012203 (2014).
- [8] K. Liu, J.E. Kollmer, K.E. Daniels, J. Schwarz, S. Henkes, Spongelike Rigid Structures in Frictional Granular Packings, *Physical Review Letters* **126**, 088002 (2021).
- [9] Y. Zhao, J. Barés, H. Zheng, J.E. Socolar, R.P. Behringer, Shear-jammed, fragile, and steady states in homogeneously strained granular materials, *Physical review letters* **123**, 158001 (2019).
- [10] K.E. Daniels, J.E. Kollmer, J.G. Puckett, Photoelastic force measurements in granular materials, *Review of Scientific Instruments* **88** (2017).
- [11] A. Abed Zadeh, J. Barés, T.A. Brzinski, K.E. Daniels, J. Dijkstra, N. Docquier, H.O. Everitt, J.E. Kollmer, O. Lantsoght, D. Wang et al., Enlightening force chains: a review of photoelasticity in granular matter, *Granular Matter* **21**, 1 (2019).
- [12] R. Sharma, A. Sauret, Experimental models for cohesive granular materials: a review, *Soft Matter* (2025).
- [13] J. Yang, X. Cai, Q. Pang, X.w. Guo, Y.l. Wu, J.l. Zhao, Experimental study on the shear strength of cement-sand-gravel material, *Advances in Materials Science and Engineering* **2018**, 2531642 (2018).
- [14] Y. Amini, A. Hamidi, E. Asghari, Shear Strength Characteristics of an Artificially Cemented Sand-Gravel Mixture (2013)
- [15] R.N. Dass, S.C. Yen, B.M. Das, V.K. Puri, M.A. Wright, Tensile stress-strain characteristics of lightly cemented sand, *Geotechnical Testing Journal* **17**, 305 (1994).
- [16] D. Li, X. Liu, X. Liu, Experimental study on artificial cemented sand prepared with ordinary portland cement with different contents, *Materials* **8**, 3960 (2015).
- [17] N. Estrada, A. Lizcano, A. Taboada, Simulation of cemented granular materials. ii. micromechanical description and strength mobilization at the onset of macroscopic yielding, *Physical Review E—Statistical, Nonlinear, and Soft Matter Physics* **82**, 011304 (2010).
- [18] Github: photoelasticity package, <https://github.com/photoelasticity>
- [19] K. Ramesh, *Developments in Photoelasticity: A renaissance* (IOP Publishing, 2021)
- [20] Photoelasticity.net: *Theoretical aspects of the photoelasticity*, <https://photoelasticity.net/photoelasticity>
- [21] B. McMillan, S.B. Dalziel, N.M. Vriend, Validation and correction of photoelastic techniques for frictional granular systems, *Measurement Science and Technology* **36**, 055212 (2025).
- [22] A. Naseer, K.E. Daniels, T.G. Murthy, Micromechanics of compressive and tensile forces in partially-bonded granular materials (2025), arXiv:2507.19214
- [23] A. Naseer, PeGS_for_cohesion (2025), https://github.com/nsrabrar/PeGS_for_Cohesion
- [24] C.L. Lee, L. McCabe, B. McMillan, A. Naseer, D. Xie, T. Brzinski, K.E. Daniels, T.G. Murthy, K. Nordstrom, Photoelastic grain solver v2.0: An updated tool for analysis of force measurements in granular materials, (*Powders and Grains*) (2025).